Workshop on Reconstruction Schemes for MR Data
17th August 2016

Magnetic Resonance MicroImaging of a Swine Infarcted Heart: Performing Cardiac Virtual Histologies

Rafael Ortiz-Ramón[1], José Manuel Morales[2], Silvia Ruiz-España[1],
Vicente Bodí[3,4], Daniel Monleón[3] and David Moratal[1]

[1] Center for Biomaterials and Tissue Engineering, Universitat Politècnica de València, Valencia, Spain

[2] Unidad Central de Investigación en Medicina, Universitat de València, Valencia, Spain

[3] Fundación de Investigación del Hospital Clínico Universitario de Valencia, Valencia, Spain

[4] Department of Medicine, Universitat de València, Valencia, Spain

Workshop on Reconstruction Schemes for MR Data
17th August 2016

This is a presentation of the work exhibited in the 37th Annual International Conference of the IEEE Engineering in Medicine and Biology Society (EMBC'15) in Milan, Italy (August 25th-29th, 2015).

R. Ortiz, J. M. Morales, S. Ruiz-España, V. Bodí, D. Monleón and D. Moratal, "Magnetic resonance microimaging of a swine infarcted heart: Performing cardiac virtual histologies," *2015 37th Annual International Conference of the IEEE Engineering in Medicine and Biology Society (EMBC)*, Milan, 2015, pp. 1584-1587.

DOI: 10.1109/EMBC.2015.7318676

Introduction — The myocardial infarction

- The myocardial infarction (MI) is the leading cause of death in developed countries.
  - MI occurs when blood flow stops to part of the heart, causing damage to the heart muscle.

- Nowadays around a 70% of patients hospitalised with MI survive the hospital phases.
  - It is necessary to control the evolution of these patients’ hearts and prevent and identify future cardiovascular risks → **CARDIAC IMAGING**

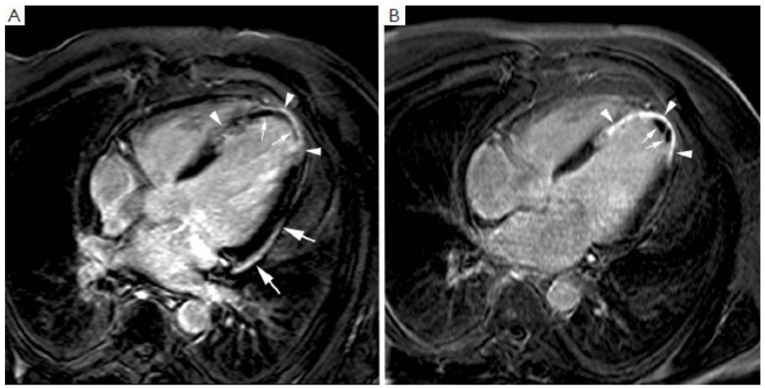

Introduction

Swine as model in cardiovascular research

⌘ <u>APPROACH → Study of medical images of a swine's infarcted heart</u>

⌘ Swine are commonly used in cardiovascular research because porcine and human hearts share important anatomic and physiologic characteristics:
- Similar size and shape
- Similar distribution of blood supply by the coronary artery

⌘ Magnetic Resonance Imaging (MRI):
- Non-invasive technique
- Strong control over the data acquisition and how it can be managed.
- Image with high precision and reliability.

Porcine Heart

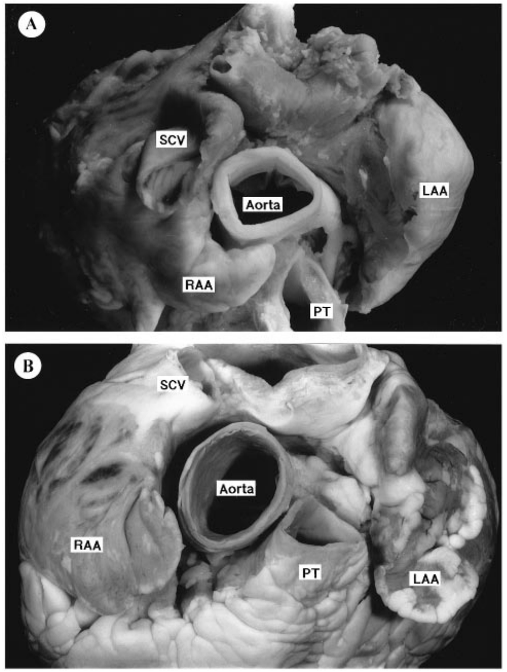

Human Heart

Objectives

⌘ Development of an intuitive software tool in MATLAB that allows a detailed study of the magnetic properties of infarcted hearts tissue by the mathematical processing of a set of Magnetic Resonance (MR) microimages of that tissue.

- Recreation of a virtual histology of infarcted heart tissue.

⌘ Preliminary stage: Work with a swine's hearts and establish a complete analysis of the conditions of the heart after an infarction

- Compare the results of the virtual histology with the results of the histopathology
- Relate the study, as a last resort, to human hearts.

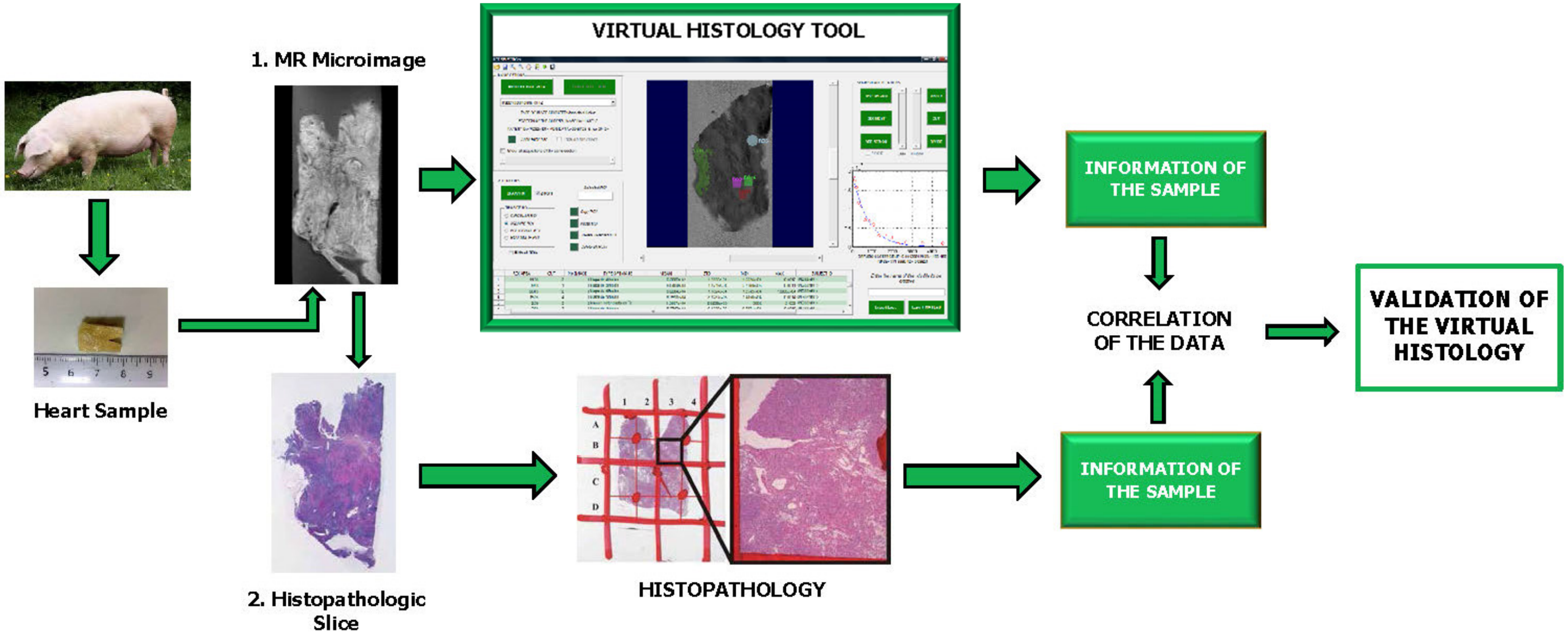

Materials and Methods

⌘ Two small samples (size 1 cm × 1.6 cm) of the infarcted heart of two different young female domestic pigs.

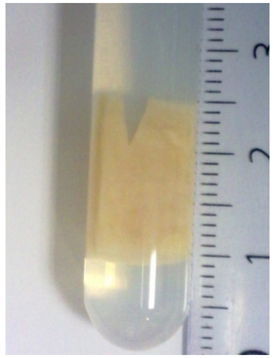

- Obtaining the images:
  1. The samples are introduced in an agarose matrix inside a tube.
  2. These tubes with the heart samples are introduced one by one in the NMR tube of the spectrometre (1 cm wide) and correctly positioned in the inside of the coil
  3. Run the required sequences in order to obtain the MR microimages.

⌘ Bruker Spectrometre ADVANCE 14 Teslas

- Acquisition of 5 types of weighted images (matrix size = 256 × 256):
  - T1-weighted reference image (TR = 500 ms; TE = 9,3 ms)
  - T2-weighted reference image (TR = 4000 ms; TE = 57,6 ms)
  - Diffusion-Weighted Images (DWI) (16 b-values)
  - T2-weighted images (TR = 2000 ms; 16 TE values)
  - T2*-weighted images (TR = 1500 ms; 12 TE values)

Materials and Methods

T1-weighted Image

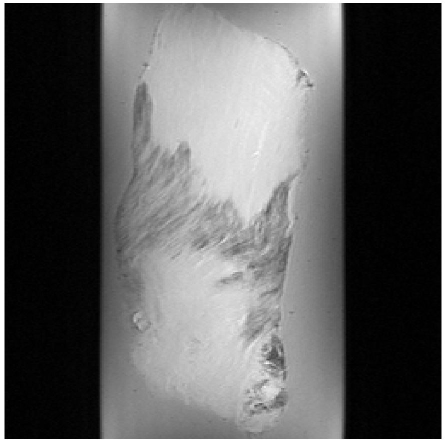

T2-weighted Image

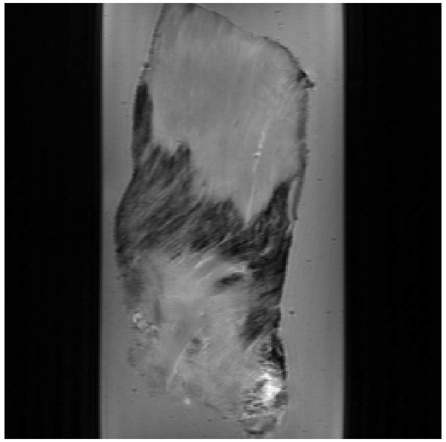

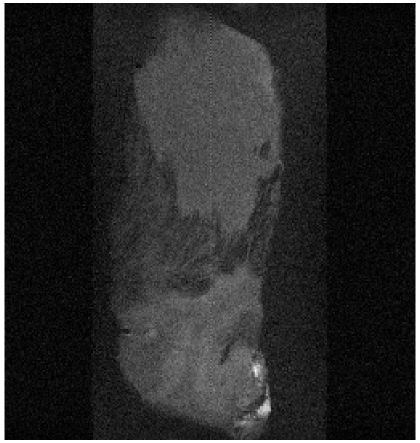

DWI
Acquisition num. 8
b-value=822.297 s/mm^2

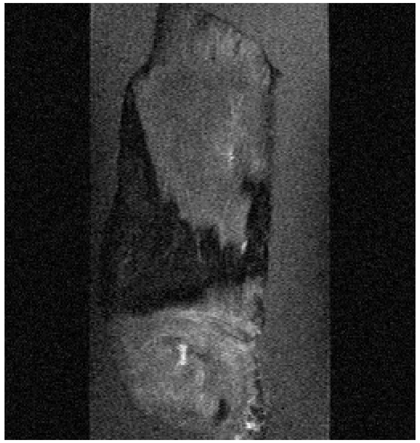

T2-weighted Image
Acquisition num. 8
TE=78.19 ms

T2*-weighted Image
Acquisition num. 8
TE=34 ms

Materials and Methods

Generating the maps: Process

⌘ The process to generate the maps consists on:

1. Analyse pixel by pixel every acquisition of each slice of the sample and store the values of the pixels.
2. Execute the fitting process of the set of values of the pixels using the values of the variable parameter, previously known.
3. Generate the map with the ADC, T2 or T2* value obtained for each pixel

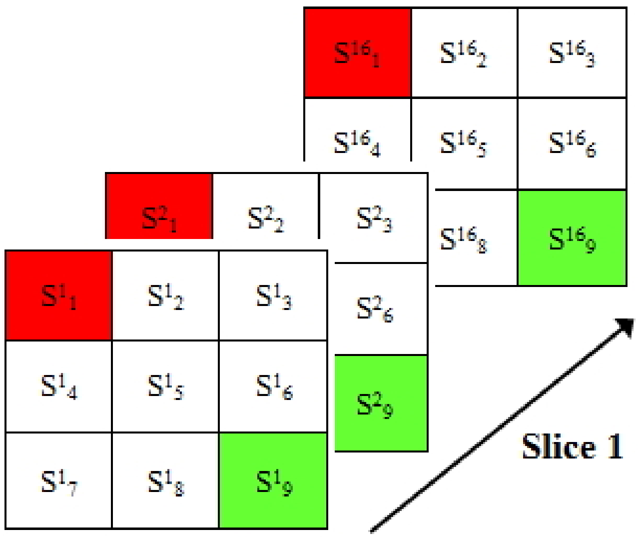

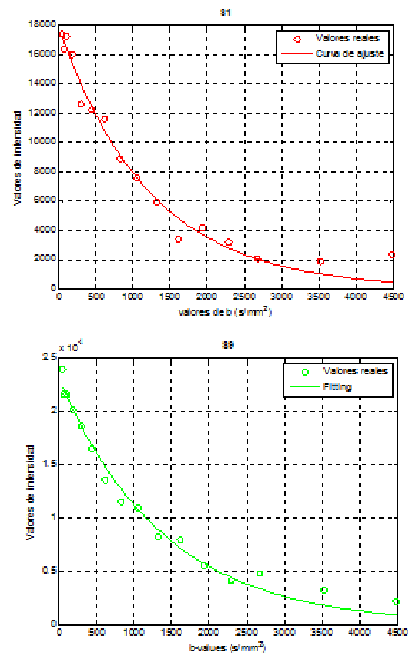

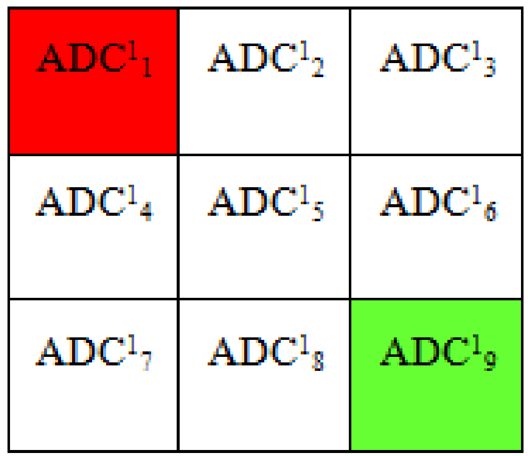

Materials and Methods

Generating the maps: Equations

- ADC map: the variable parameter is the *b-value* (s/mm^2)
  - Mono-Exponential $$S(b) = S_0 e^{-bD}$$
  - Bi-exponential $$S(b) = S_0[\xi e^{-bD_f} + (1-\xi)e^{-bD_s}]$$
- T2 and T2* maps: the variable parameter is the Time of Echo TE (s)
  - Mono-exponential $$S(TE) = S_0 e^{-\frac{TE}{T2}}$$

Results

Structure of the Graphical User Interface

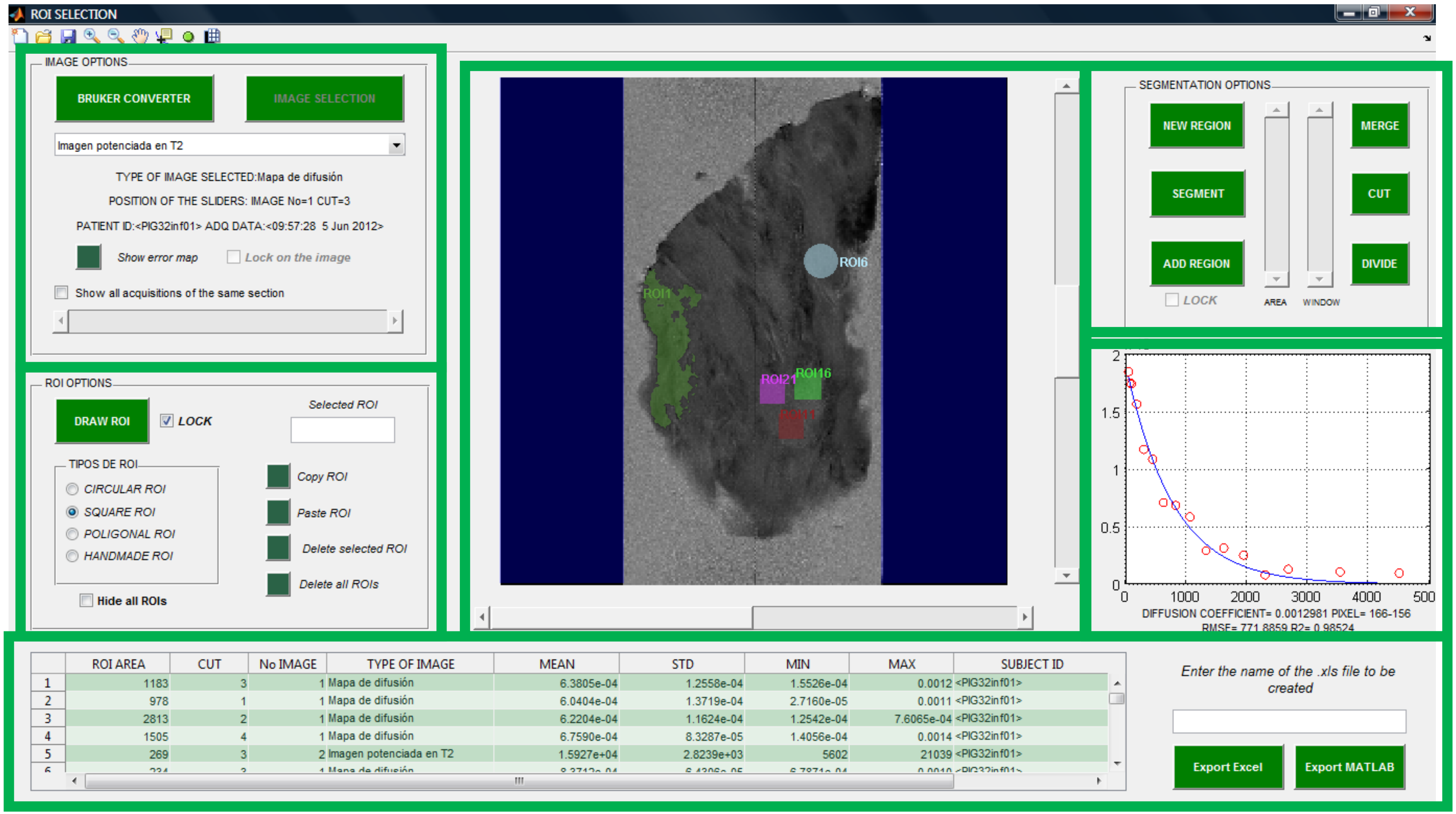

Results

Image Options
Types of images

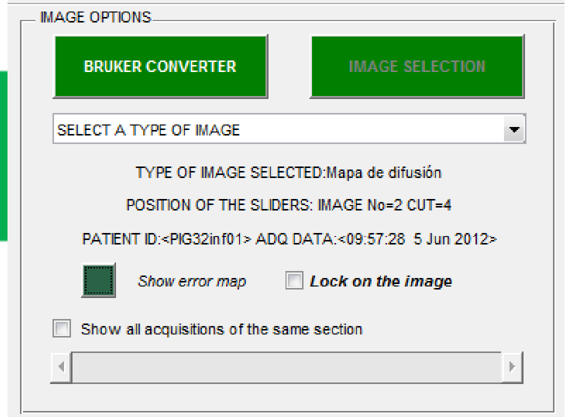

⌘ The images are classified in two groups:

- GROUP A: Reference images that do not need a fitting process:
  - T1-weighted image
  - T2-weighted image

- GROUP B: Images that need a fitting process in order to generate a map:
  - DWI (16 acq.) → ADC map
  - T2-weighted images (16 acq.) → T2 map
  - T2*-weighted images (12 acq.) → T2* map

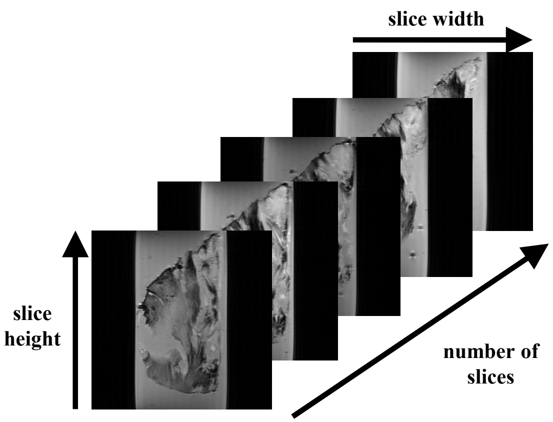

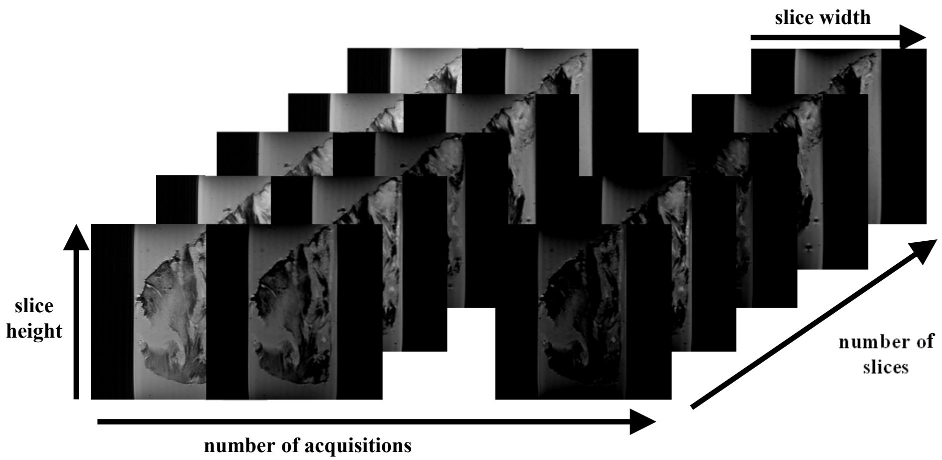

⌘ The tool implements four methods in order to fit the data.

Results

Image Options
Maps

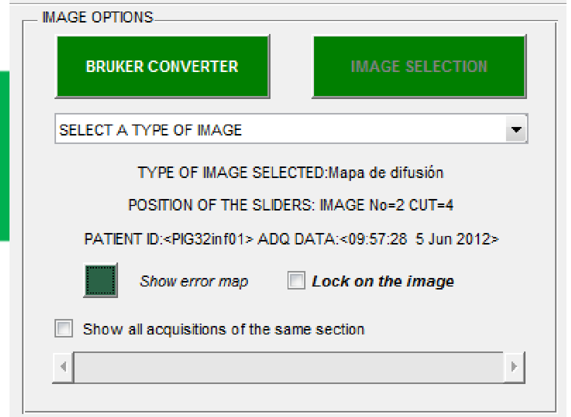

- Method 1: **High resolution exponential.**
  - Curve fitting using nonlinear regression, with previous models

- Good fitting and graphical results for many cases but improvable

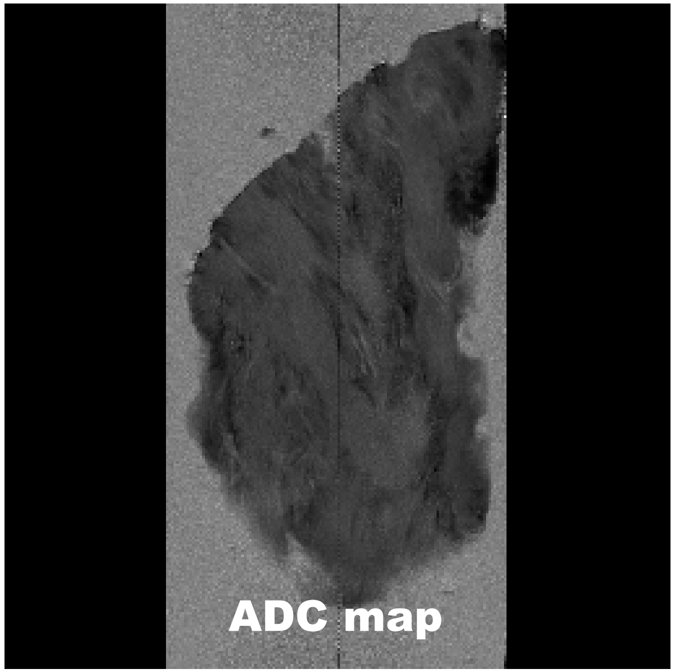

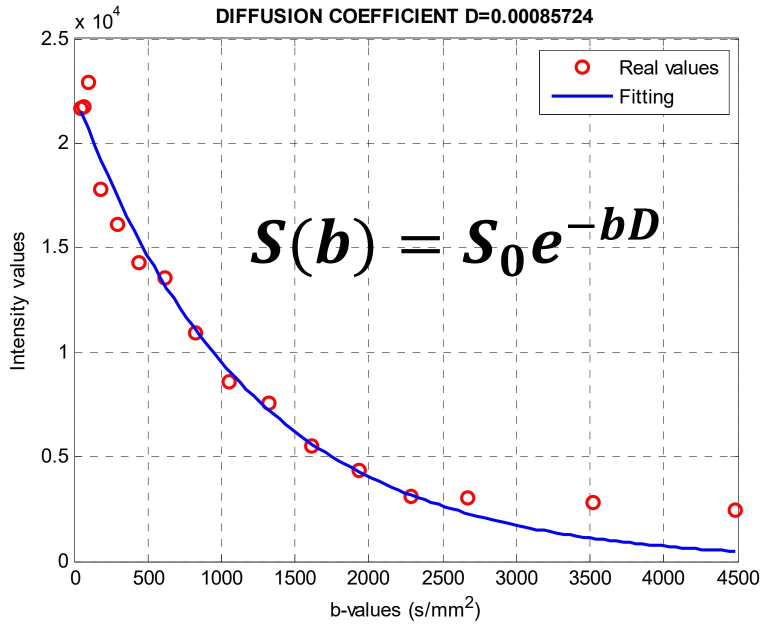

Results

Image Options
Maps

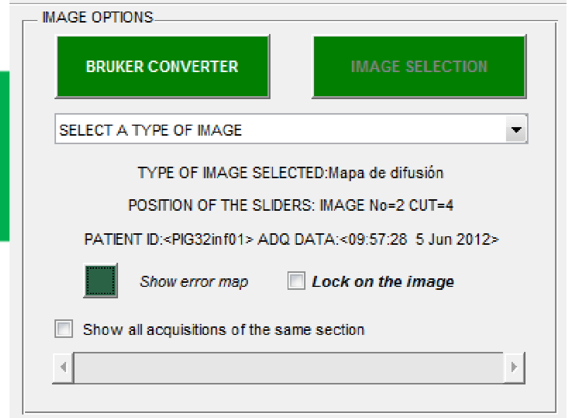

- Method 2: **Low resolution exponential.**
  - Linearization of exponential equation → Linear regression.

$$S' = \log S(b) = \log S_0 + (-bD) = S_0' - bD$$

- Worst fitting results but faster operations

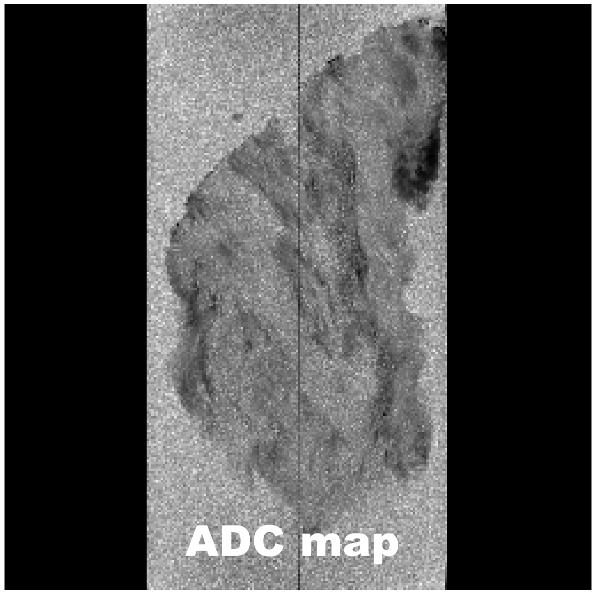

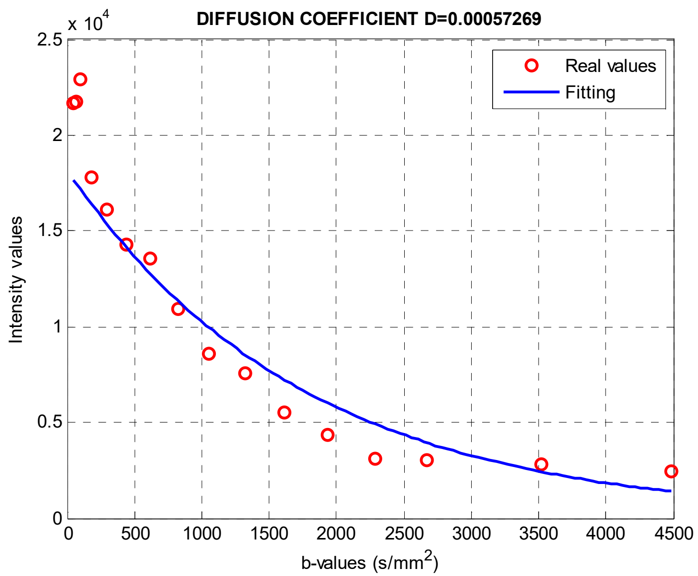

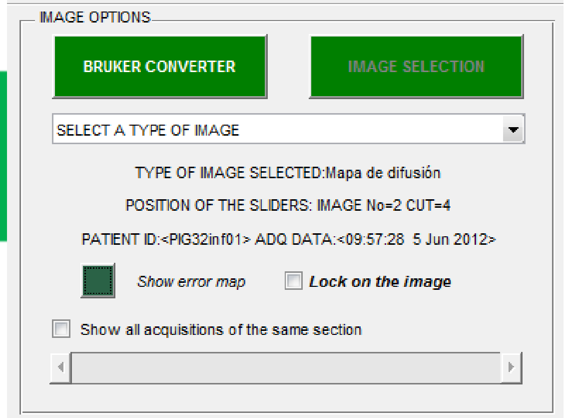

Results

Image Options
Maps

⌘ Method 3: **Exponential with baseline.**

➢ Compensation of the biexponential behavior of some curves by introducing a baseline → Nonlinear regression using customized models

$$S(b) = S_0[1 + \xi e^{-bD}]$$

⌘ Better approach (reliable data and image) but slower operations

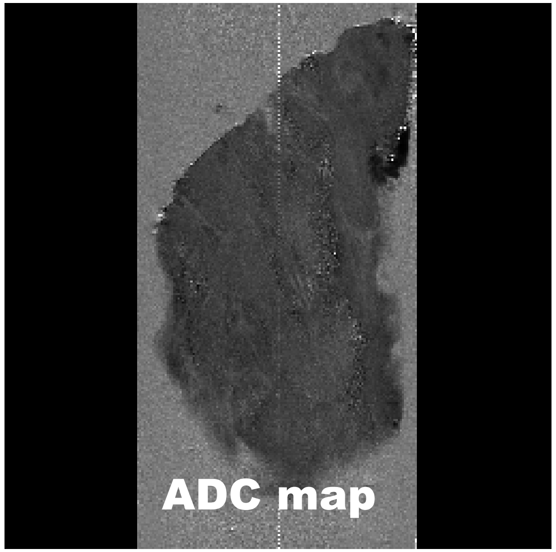

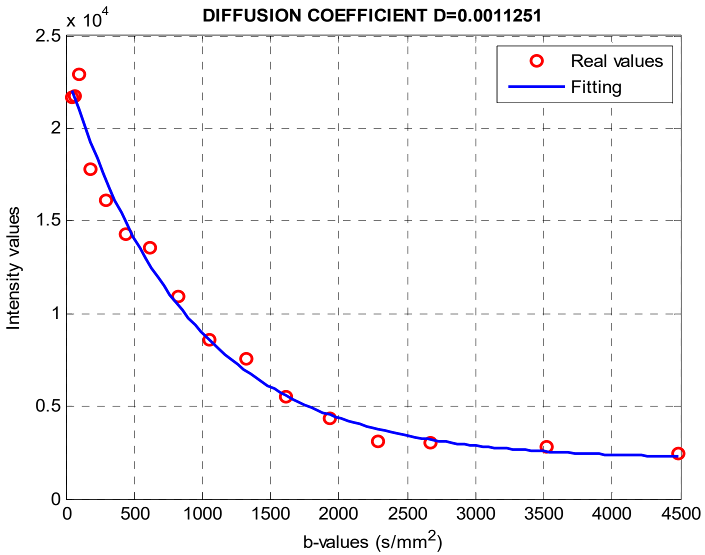

Results

Image Options
Maps

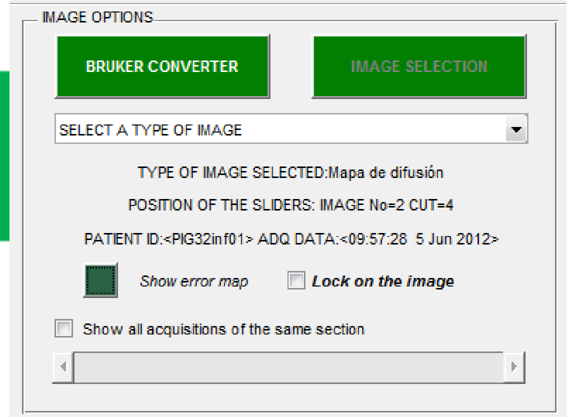

- Method 4: **Biexponential.**
  - Curve fitting using nonlinear regression, with previous models

- Perfect fitting results but problems with the resulting image

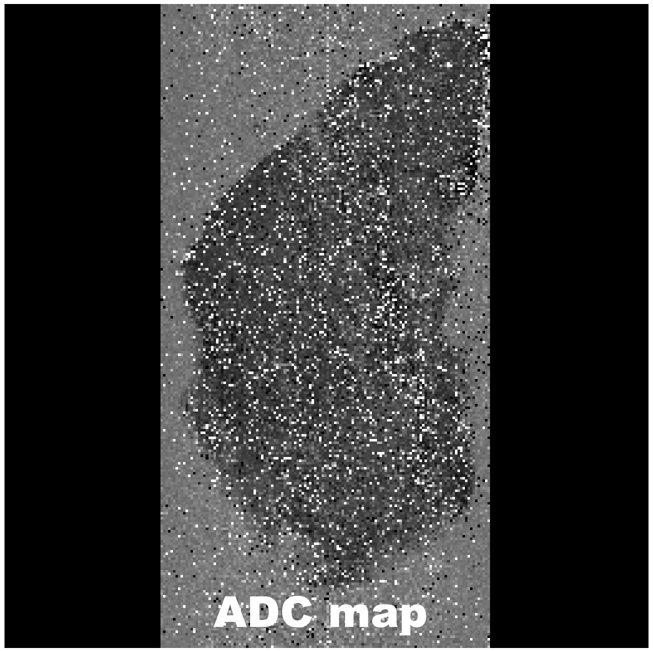

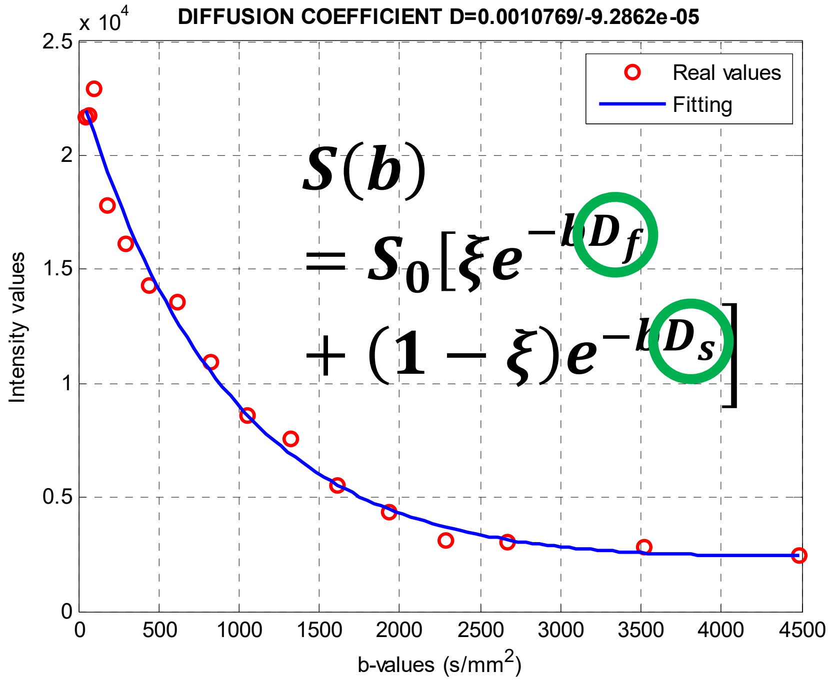

$$S(b) = S_0[\xi e^{-bD_f} + (1-\xi)e^{-bD_s}]$$

Results

Image Options
Maps

High resolution exponential

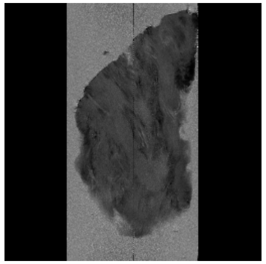

11.81 min/slice *

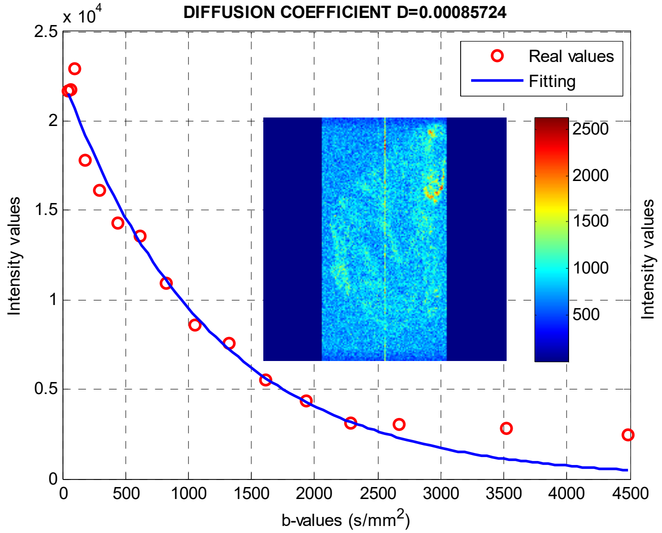

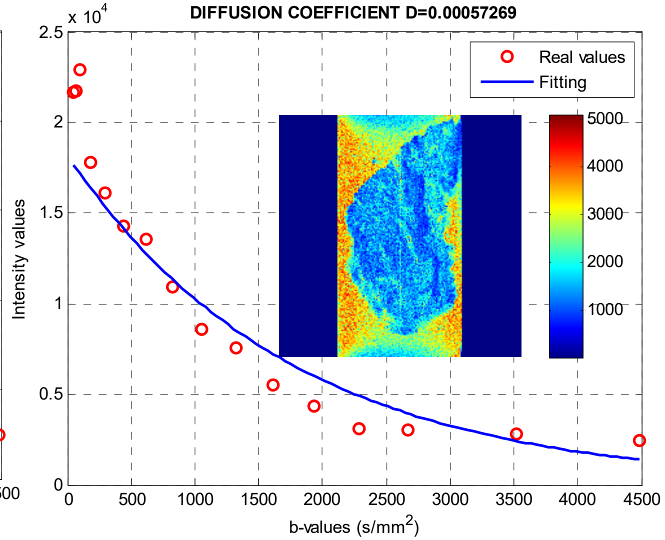

Low resolution exponential

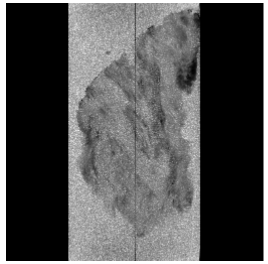

1.41 min/slice *

22.45 min/slice *

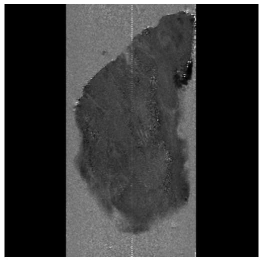

Exponential with baseline

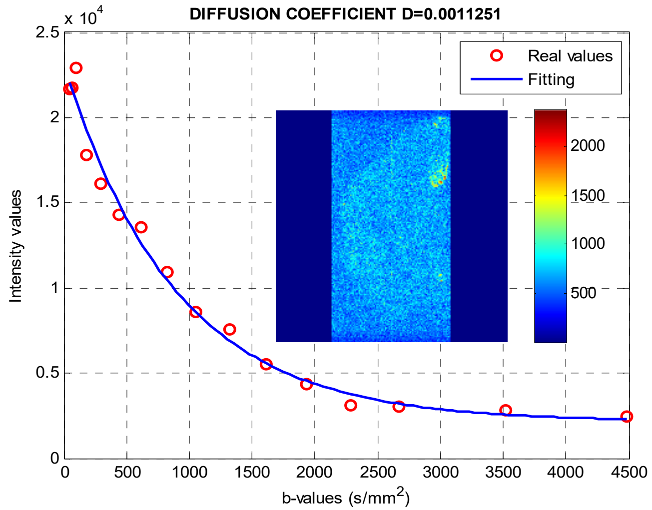

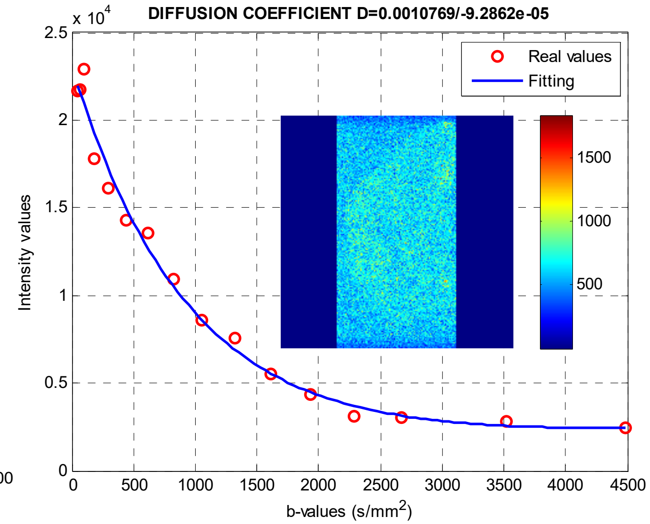

18.91 min/slice *

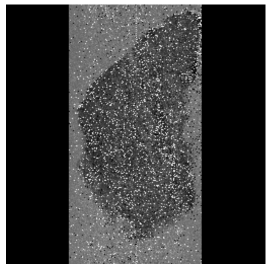

Biexponential

*** Tested with a Dell Computer with Intel Core i7-4790 Processor, 16 GB of RAM and Windows 7 Professional 64 bit**

Results

Image Options
Maps

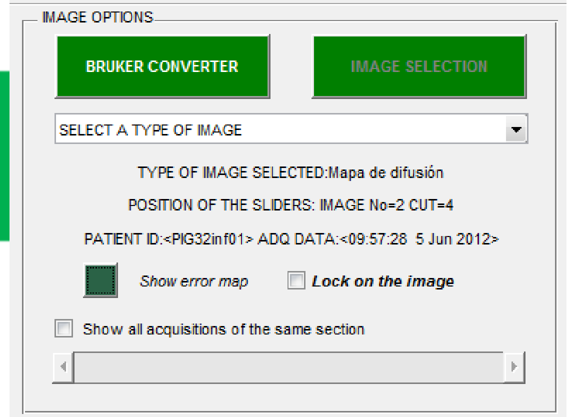

- The duration of the process is very variable:
  - It depends on the selected fitting method and the power of the computer.
  - Generally SLOW.

- **Downsampling**
  - Decimate the image: fitting method applied to a reduced number of pixels and the rest of the pixels reconstructed by interpolation.
  - Decrease of the quality of the map but faster process

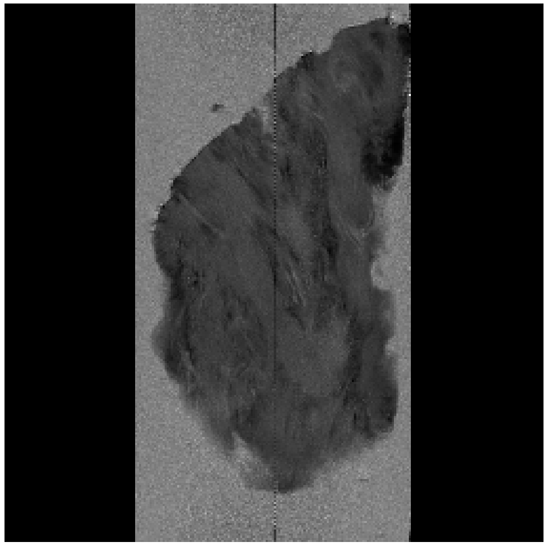

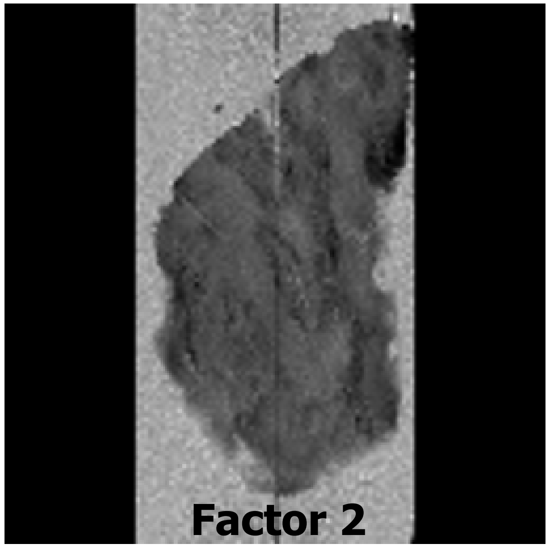

Factor 2

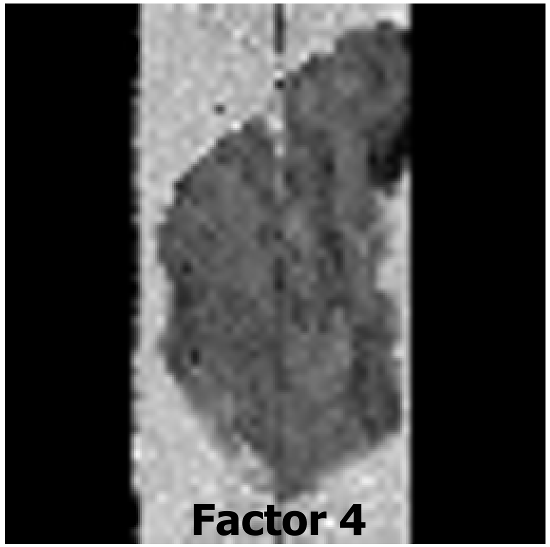

Factor 4

Results

Image Options
Error Maps

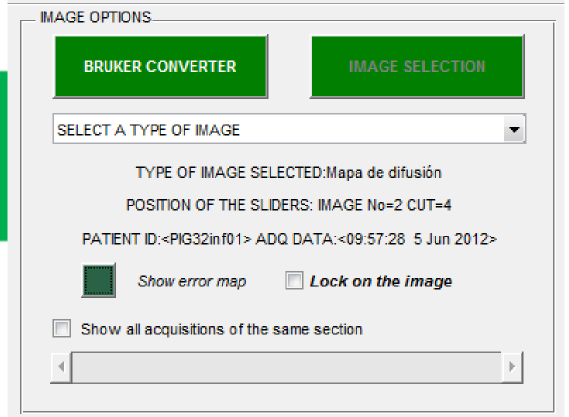

⌘ Color-based Error Maps

- ➢ Wide view of the differences between the original data and its approximated curve
- ➢ Each pixel of the Error Map represents the error caused when applying the fitting on the respective data.

○ R-squared error map:

$$SST = \sum_{i=1}^{n} (y_i - \bar{y})^2 \qquad SSR = \sum_{i=1}^{n} (\hat{y}_i - \bar{y})^2 \qquad R^2 = \frac{SST}{SSR}$$

○ RMSE error map:

$$RMSE = \sqrt{MSE} = \sqrt{\frac{1}{n}\sum_{i=1}^{n} (\hat{y}_i - y_i)^2}$$

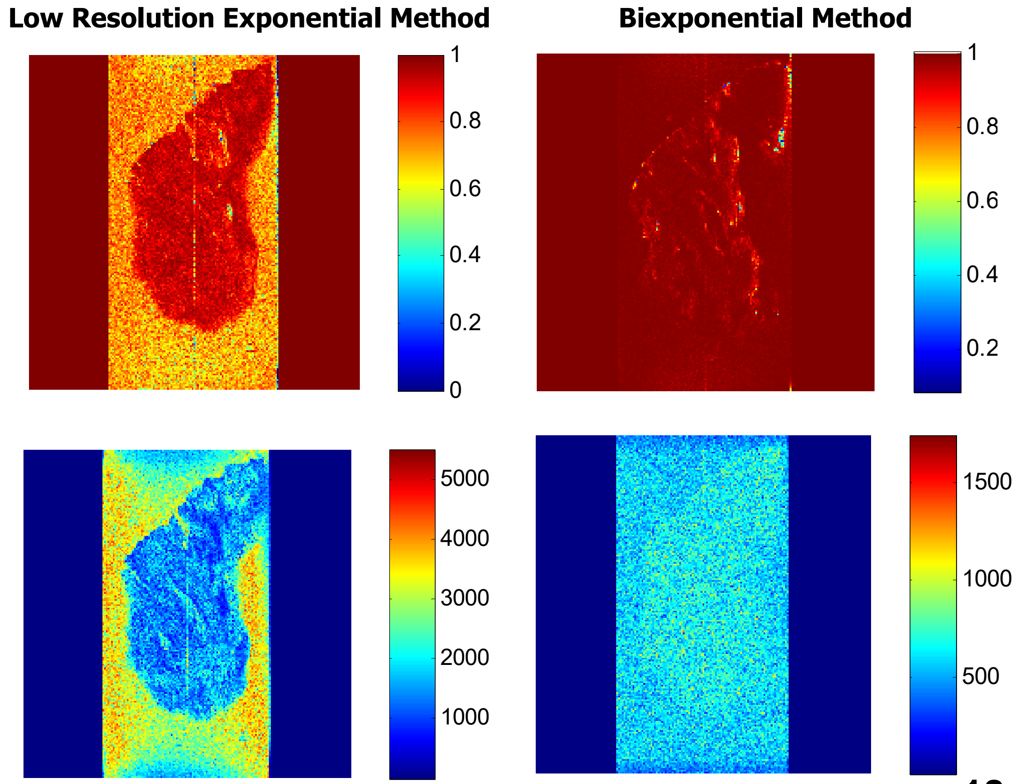

Results

Image Options
Error Maps

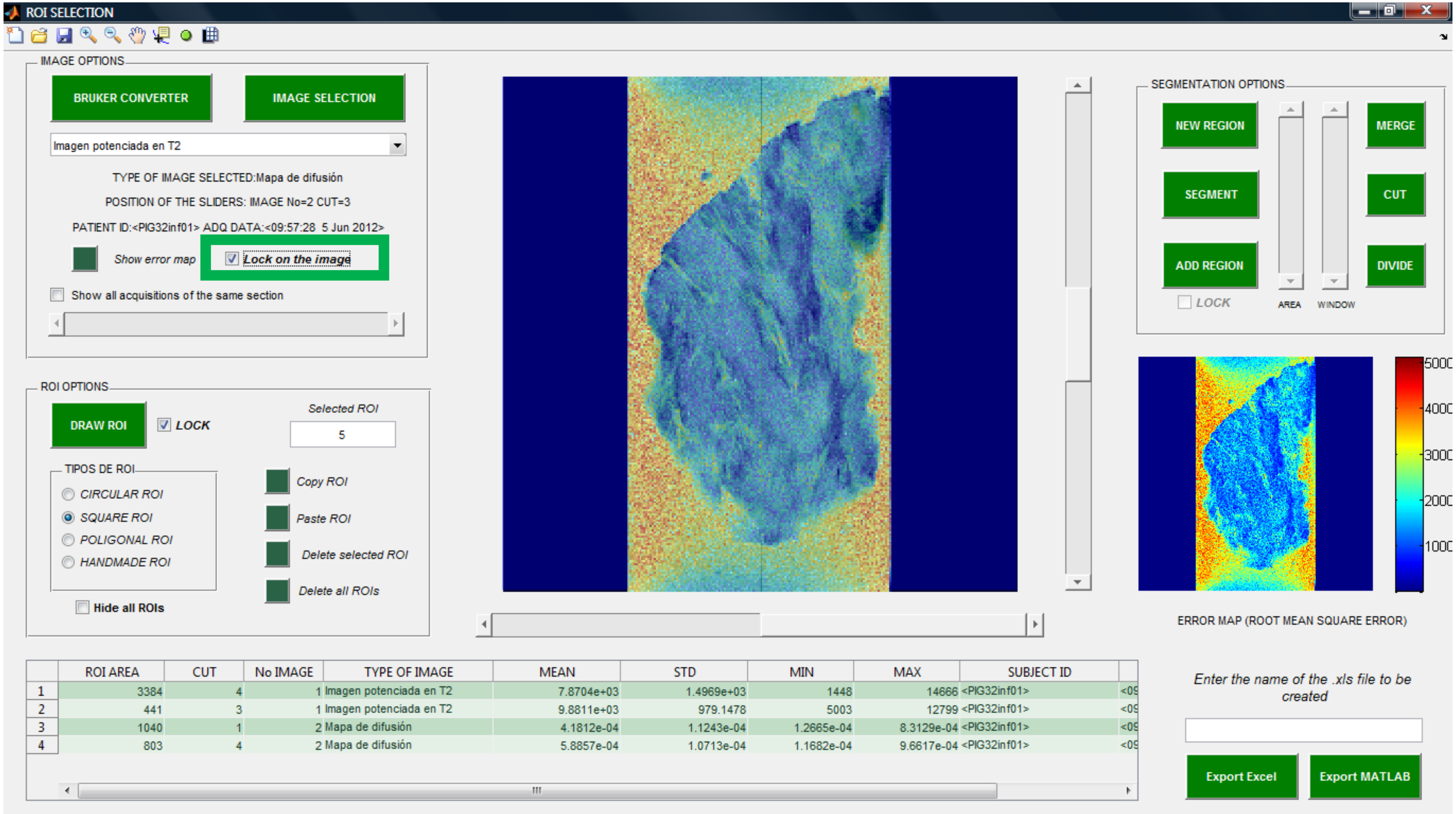

Results

ROI options

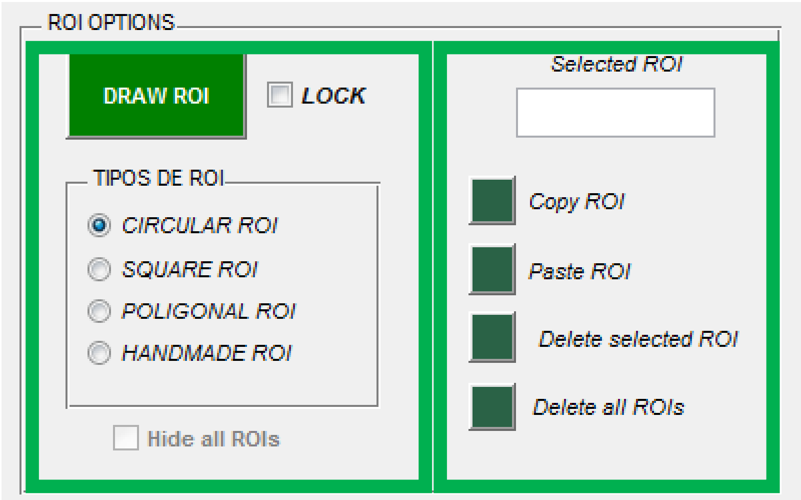

- ⌘ ROI area, in number of pixels
- ⌘ Slice number
- ⌘ MR microimage number
- ⌘ Type of image
- ⌘ Mean value of the pixels of the ROI
- ⌘ Standard deviation of the pixels of the ROI
- ⌘ Minimum of the ROI
- ⌘ Maximum of the ROI
- ⌘ Identifier of the sample
- ⌘ Acquisition date of the sample

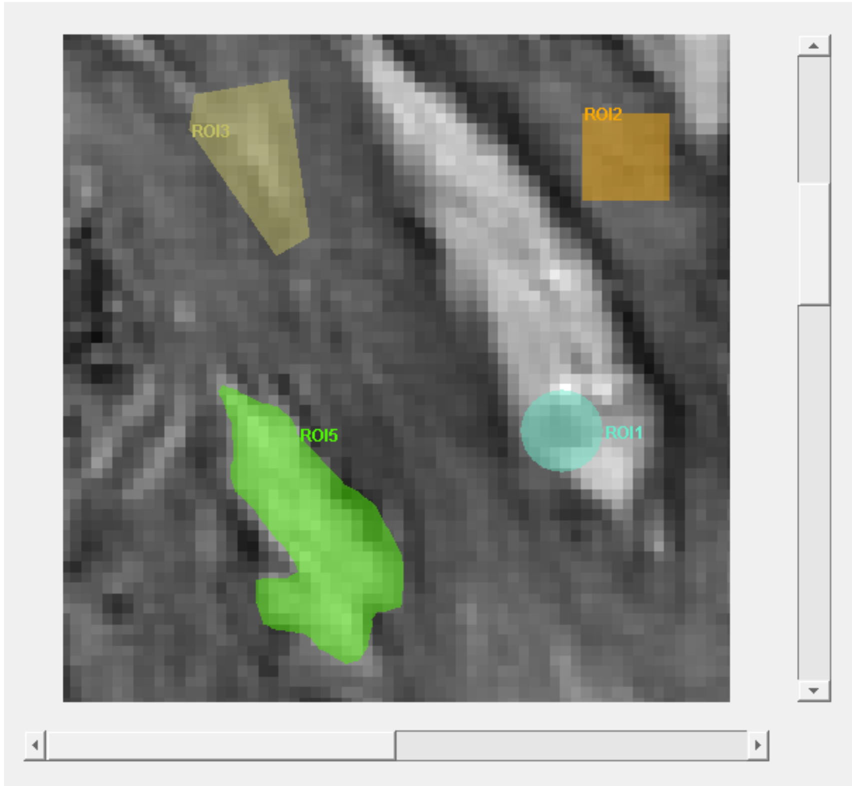

- Smart and semiautomatic selection of regions
  - **Region-growing method:** Region growing criterion based on an "analysis window"

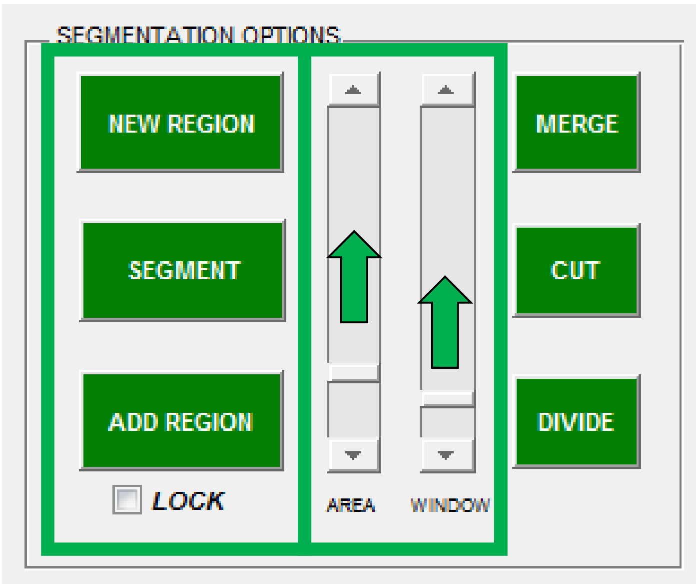

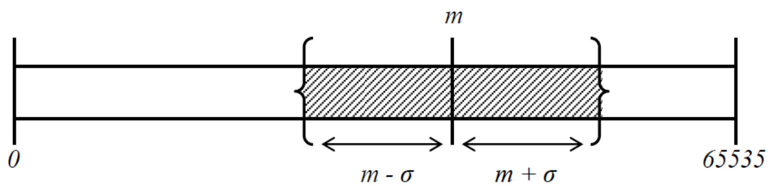

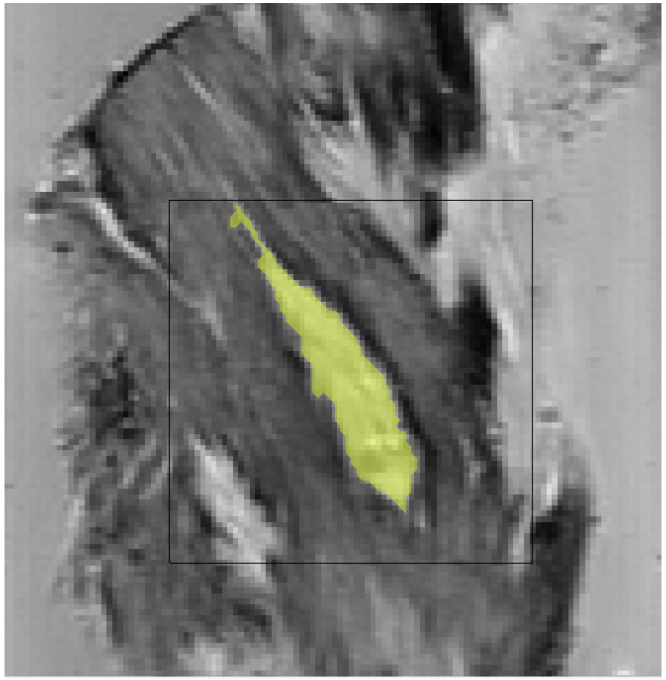

Results

Segmentation Options

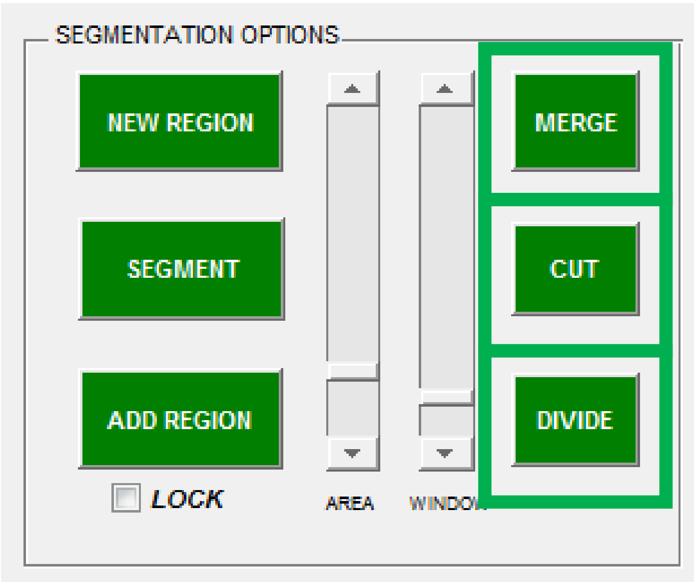

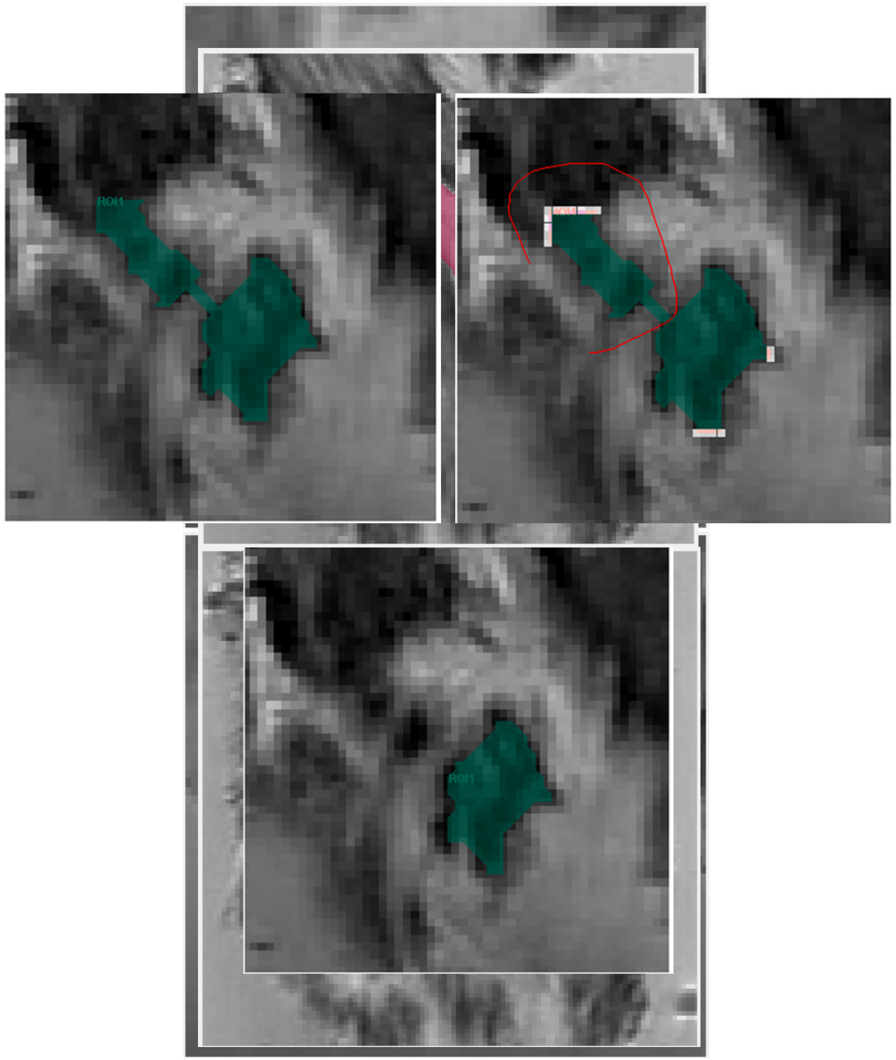

Conclusions

- Development of an intuitive tool to perform virtual histologies by analyzing MR microimages of swine infracted heart samples.
  - Processing of 5 type of MR microimages.
  - Implementation of 4 types of exponential fitting methods in order to obtain ADC, T2 and T2* maps.
  - Evaluation of the fitting results using Error maps.
  - Image analysis using ROIs.
  - Smart selection of regions using segmentation methods.

- The results have been tested comparing them with previously validated virtual histologies analysed with *Paravision* (Bruker Biospin, Ettlingen, Germany).

- The tool is currently being used by medical personnel of the Molecular Imaging and Metabolomics Group (UIMM) of the Fundación de Investigación of the Hospital Clínico Universitario de Valencia (Valencia, Spain).

Workshop on Reconstruction Schemes for MR Data
17th August 2016

Magnetic Resonance MicroImaging of a Swine Infarcted Heart: Performing Cardiac Virtual Histologies

Rafael Ortiz-Ramón[1], José Manuel Morales[2], Silvia Ruiz-España[1], Vicente Bodí[3,4], Daniel Monleón[3] and David Moratal[1]

[1] Center for Biomaterials and Tissue Engineering, Universitat Politècnica de València, Valencia, Spain

[2] Unidad Central de Investigación en Medicina, Universitat de València, Valencia, Spain

[3] Fundación de Investigación del Hospital Clínico Universitario de Valencia, Valencia, Spain

[4] Department of Medicine, Universitat de València, Valencia, Spain

INCLIVA Instituto de Investigación Sanitaria

Universitat de València

Centro de Biomateriales e Ingeniería Tisular Universidad Politécnica de Valencia

Universitat Politècnica de València